IEEE Open Access Journal of
Power and Energy

Received 1 December 2020; revised 17 March 2021; accepted 5 April 2021.
Date of publication 7 April 2021; date of current version 19 April 2021.

Digital Object Identifier 10.1109/OAJPE.2021.3071692

Examination of Composite Load and Variable Frequency Drive Air Conditioning Modeling on FIDVR

ADRIANA CISCO SULLBERG[1] (Student Member, IEEE), MENG WU[1] (Member, IEEE), VIJAY VITTAL[1] (Life Fellow, IEEE), BO GONG[2] (Senior Member, IEEE), AND PHILIP AUGUSTIN[2] (Member, IEEE)

[1]School of Electrical, Computer and Energy Engineering, Arizona State University, Tempe, AZ 85287 USA
[2]Salt River Project, Scottsdale, AZ 85251 USA

CORRESPONDING AUTHOR: V. VITTAL (vijay.vittal@asu.edu)

This work was supported by the Salt River Project.

ABSTRACT Fault induced delayed voltage recovery (FIDVR) is a credible concern in power systems with high penetration of single-phase air conditioner loads. Power system planning studies use dynamic load models, such as the Western Electricity Coordinating Council (WECC) composite load model CMPLDW to examine FIDVR in power systems. The behavior of modern variable frequency drive (VFD) air conditioners to voltage drops is not the same as traditional one- or two-speed air conditioning systems. This paper investigates the impact of increasing VFD air conditioner penetration within a power system on FIDVR events, by first modeling VFD air conditioners as a separate load and then as a power electronic component within the CMPLDW model. Simulation results show that increasing the penetration of VFD driven air conditioners decreases the post-fault voltage sag, recovery time, and number of customers interrupted by undervoltage load shedding.

INDEX TERMS Air conditioning, dynamic load modeling, fault induced delayed voltage recovery, variable frequency drives.

NOMENCLATURE

A_{new}	Age less than which an air conditioner is considered new.
A_{rep}	Age at which an air conditioner is replaced.
α_{VFD}	Penetration of VFD air conditioners among new air conditioners.
Fma_0	Fraction of the load modeled as Motor A in CMPLDW in the base case.
Fma	Fraction of the load modeled as Motor A in CMPLDW in the VFD penetration case study.
Fmb_0	Fraction of the load modeled as Motor B in CMPLDW in the base case.
Fmb	Fraction of the load modeled as Motor B in CMPLDW in the VFD penetration case study.
Fmc_0	Fraction of the load modeled as Motor C in CMPLDW in the base case.
Fmc	Fraction of the load modeled as Motor C in CMPLDW in the VFD penetration case study.
Fmd_0	Fraction of the load modeled as Motor D in CMPLDW in the base case.
Fmd	Fraction of the load modeled as Motor D in CMPLDW in the VFD penetration case study.
Fmd_i	Percentage of load which is single-phase motor load at bus i.
Fel_0	Fraction of the load modeled as power electronic in CMPLDW in the base case.
Fel	Fraction of the load modeled as power electronic in CMPLDW in the VFD penetration case study.
$Frcel_0$	Fraction of the power electronic load which can reconnect after voltage sags, in the base case.
$Frcel$	Fraction of the power electronic load which can reconnect after the voltage sags in the VFD penetration case study.
$N_{H,i}$	Total number of homes at bus i.
$N_{H_y,i}$	Number of homes built in year y at bus i.
$N_{H_{new}}$	Number of homes with new air conditioners.
P_{1_0}	Load represented by CMPLDW in the base case.

P_1	Load modeled as CMPLDW in the VFD penetration case study.
P_2	VFD air conditioner load modeled as LD1PAC in the VFD penetration case study.
$P_{load,i}$	Real power load at bus i.
ρ_i	Percentage of homes with new air conditioners at bus i.
$\rho_{VFD,i}$	Percentage of new air conditioners which are VFD driven at bus i.
ρ'_{VFD}	Percentage of VFD driven air conditioners in the power system.
y	A given year.

I. INTRODUCTION

FIDVR is of concern in power systems with high penetration of single-phase air conditioner loads. When the voltage drops following a fault, and stalling occurs, there is an increase in active and reactive power consumed by the motor. Single-phase air conditioners stall when the electrical torque developed in the motor is not adequate to overcome the constant mechanical torque required by the air conditioner compressor. The high reactive power demand during the stalling may prevent the post-fault bus voltage from recovering to nominal values.

A. DYNAMIC LOAD MODELING

The North American Electric Reliability Corporation (NERC) Reliability Standard TPL-001-4 Requirement R2.4.1 requires the use of dynamic load models of induction motors in planning studies and suggests the use of an aggregate dynamic load model [1]. WECC developed the CMPLDW to model the most common consumer loads in an aggregated fashion [1], [2]. The CMPLDW model contains four types of induction motors (typically with Motors A-C representing three types of three-phase motors and Motor D representing the single-phase motor), the electronic load and the static load. While easing the modeling burden by not modeling each load type independently, the WECC CMPLDW model is complex with a large number (121) of user-defined parameters to characterize the loads [3]. Many of the parameters related to component protection functions have been determined by conducting laboratory tests and reviews of manufacturer literature for devices reported being used during end-use surveys and are typically left unchanged by users. A smaller number of parameters are related to load composition and are meant to be modified based on utility feeder-specific data, such as *Fma, Fmb, Fmc, Fmd,* and *Fel*. Both Pacific Northwest National Laboratory (PNNL) and the Electric Power Research Institute (EPRI) have developed software to assist CMPLDW model users adjust model parameters if there is insufficient feeder-specific data available to system planners [4], [5]. The load modeling tools rely on user input of season, operating hour, climate zone, and load type percentages. NERC published a list of typical CMPLDW parameter values and provided guidance regarding the specific parameters that need to be tuned [6].

In positive sequence power system simulation tools such as GE PSLF, single-phase motor dynamics, unlike those of three-phase motors, cannot be represented by a suitable dynamic model. Instead, a performance model is used. The performance model is a state-model which uses algebraic equations to calculate motor power in two states: a run state and a stall state. Motor protection is also modeled, which includes the effect of disconnecting the motor and having zero output power. The motor state is characterized by user-defined CMPLDW parameters.

B. VFD DRIVEN AIR CONDITIONERS

EPRI has performed laboratory tests of various residential air conditioner types, including VFD driven air conditioners, aiming to improve Motor D parameter tuning [7]. While testing residential air conditioners, EPRI found that the VFD driven air conditioners disconnect when the voltage at the motor terminal drops to 0.75-0.70 pu, and do not reconnect for *several minutes*. This is a significant departure from the behavior of one- and two-speed air conditioners. These findings are incorporated into the modeling proposed in this paper by changing the voltage trip and reconnection settings and eliminating stalling for VFD driven air conditioners.

EPRI has presented an aggregate VFD model in [8] and [9] to represent an aggregation of three-phase industrial VFD loads. The model is not yet available in commercially available positive sequence dynamic simulation packages. The VFDs tested by EPRI to develop the aggregate model were three-phase and, in general, larger in horsepower rating than the single-phase air conditioner EPRI tested in [7].

The NERC-recommended Motor D parameters reflect the behavior of one- and two-speed air conditioners, not VFD driven air conditioners. NERC documentation and software manuals do not specifically address modeling VFD driven air conditioners, and utilities may not have end-use information on VFD driven air conditioners in their service territory. Appropriately tuning CMPLDW parameters to model residential VFD driven air conditioners can lead to more realistic study results. Hence, in this paper, the data provided in [7] based on testing VFD driven air conditioners is utilized to appropriately tune the CMPLDW model such that the VFD driven air conditioners trip when voltage lowers to 0.75-0.70 pu and do not reconnect. The analysis presented in this paper shows the benefits of VFD driven air conditioners on reducing FIDVR's impact on the system, which can steer system upgrades and inform utility consumer rebates for variable speed air conditioners – i.e. where to invest utility capital.

VFD driven air conditioners are power electronic interfaced and can be represented by the power electronic load representation in the CMPLDW model. The power electronic representation is a constant active and reactive power load which linearly decreases between user-defined voltages V_{tr1} to V_{tr2}, at which point 100% of the power electronic load is disconnected. This paper presents a methodology for representing VFD driven air conditioning as a power electronic

load when all air conditioning has been hitherto considered one- and two- speed, as represented by Motor D.

Presently, there are some limitations on the penetration of VFD driven air conditioners. The initial investment cost of VFD air conditioners is higher than that of one- or two-speed air conditioners. While the long-term savings of the VFD driven air conditioner will bring a return on investment, it may take years to do so. If a consumer is unable to afford the initial investment cost or is not planning to continue living in the home until the investment is returned in savings, a one- or two-speed air conditioner is more likely to be installed.

Presently, there are no residential VFD driven packaged air conditioner units on the market. Packaged units are ones in which all components of the air conditioner are manufactured in one single metal package in a factory, and installed on the exterior of a house, typically on the roof [9]. Smaller homes, homes without basements, and homes with limited or no crawl space are most likely to have packaged air conditioning units. A split air conditioning system is one in which the compressor and condenser are in one metal unit installed on the exterior of a house, and the evaporator and air handling unit is in the interior of a house, often in a crawl space or basement. It is not economical or always feasible to replace a packaged unit with a split system unit. It is possible to retrofit some packaged units with VFDs, however data on the practice is not available [10], [11].

VFDs are a relatively new technology in residential air conditioning. Considering the present and future reasonable penetration of VFD driven air conditioners in residential applications a range of α_{VFD} from 0% to 90% is chosen for this study. Presently, the range of 15% to 30% of new air conditioners being VFD driven is assumed to be reasonable. The availability and affordability of VFD driven residential air conditioners and regulatory mandates to use VFD driven residential air conditioners may drive the penetration of new VFD driven air conditioners to be greater than 30%. The above practical concerns are taken into consideration when modeling future VFD penetration scenarios in this paper.

The rest of this paper is organized as follows: Section II presents background on single-phase air conditioning modeling using a performance model. Section III presents the proposed methodology for modeling VFD driven air conditioners as a load distinct from one- and two-speed air conditioners (Motor D). Section IV present the results of case studies. Section V presents the concluding remarks.

II. SINGLE-PHASE AIR CONDITIONER MODELING

Fig. 1 shows the one-line diagram of the CMPLDW model. The model of the single-phase motor (Motor D) within the CMPLDW representation is a performance model. In GE PSLF software, the single-phase motor model, "uses essentially the same model as the LD1PAC model" [3]. The fraction of the load to be represented using Motor D in CMPLDW is determined by the parameter *Fmd*. LD1PAC and Motor D in CMPLDW model compressor motor stalling and reconnection as well as three internal tripping mechanisms:

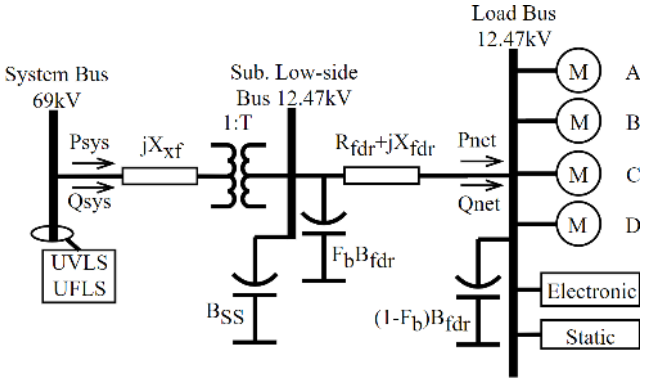

FIGURE 1. **One-line diagram of the CMPLDW model [3].**

contactor tripping, undervoltage relay protection, and thermal overload protection.

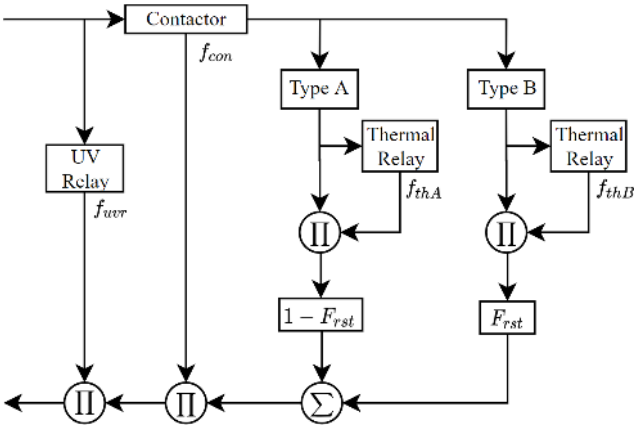

FIGURE 2. **Motor D performance model block diagram [3].**

A. STALLING

Fig. 2 shows the block diagram of the single-phase motor performance model. The single-phase motor in CMPLDW and LD1PAC stalls when the voltage at its terminals falls below V_{Stall} for T_{Stall} seconds, at which point it is represented as a constant impedance load of $R_{Stall} + jX_{Stall}$. If the voltage recovers above V_{rst} for T_{rst} seconds, a fraction of the load, F_{rst}, restarts. F_{rst} is used to split the single-phase motor load into two types, type A and type B. The type A motors are not allowed to restart after stalling, and the type B motors are allowed to restart.

B. THERMAL PROTECTION

Fig. 3 shows the thermal protection tripping scheme in the CMPLDW and LD1PAC models. When motors represented as type A or type B are stalled, the thermal overload protection scheme is then modeled. The current and R_{Stall} parameter of each set of motors is used to determine a motor temperature.

The motor heating is calculated by integrating the loss I^2R_{Stall} with a time constant of T_{TH}. The load linearly trips

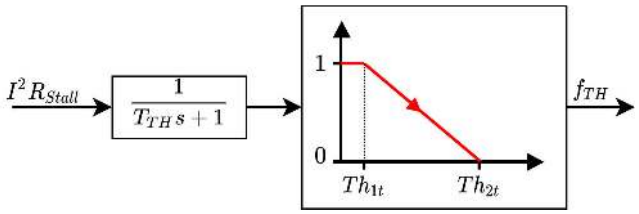

FIGURE 3. **Motor D thermal protection tripping scheme [12].**

from temperatures Th_{1t} to Th_{2t}, at which point 100% of that motor load is tripped. This calculation and the associated procedure are performed independently for type A and type B motors. This portion of the model represents the overload protection common in motor starters. The fraction of type A and type B motors which are not tripped is output as f_{THA} and f_{THB}, respectively.

Motor starters typically consist of an electromagnetic contactor in series with an overload device. In small motors, overload devices are usually bimetallic strips or solder-pots in series with the motor [6]. Both bimetallic strips and solder-pots operate over an electrically long period of time, on the order of many seconds to minutes. Overloads and thermal protection, despite operating due to elevated motor current, are not the same as overcurrent protection, which operates in a much faster time frame and protects against electrical faults.

III. VFD AIR CONDITIONER MODELING METHODOLOGY

The heavy summer load power flow and dynamic data for a real utility, and home age information for the homes in the utility's service area were used to study FIDVR events. Within a power system of 24114 buses and 4400 generators, the studied system is comprised of 746 buses and 124 generators. There are 316 load buses at 69kV modeled with CMPLDW. Discounting industrial facilities and power plant auxiliary loads, there are 264 load buses at 69kV modeled with CMPLDW. Load type and home age data was available for 254 of those 69kV load buses with CMPLDW models. The home age data includes the number of homes built each year for each 69kV feeder transformer from 1955 to 2019.

The US Department of Energy estimates that the average life cycle of residential air conditioners is 15 to 20 years [14]. Due to the very high temperatures experienced in the summer in the utility's service territory, it is assumed that residential air conditioners in the area will have a higher duty cycle and therefore a shorter lifespan. A life span of 15 years is chosen in estimating the number of new air conditioners in the service territory. A ''new'' air conditioner is defined as one that is less than 5 years old. The percentage of new air conditioners for a given 69kV bus, ρ_i, is calculated as

$$\rho_i = \frac{N_{H_{new},i}}{N_{H,i}} \tag{1}$$

$$N_{H,i} = \sum_{y=1955}^{2019} N_{H_y,i} \tag{2}$$

$$N_{H_{new},i} = \sum_{y=1955}^{2019} N_{H_y,i} x_y \tag{3}$$

where

$$M_y := (2019 - y) \bmod A_{rep} \tag{4}$$

$$x_y := \begin{cases} 1 & if\ M_y \le A_{new} \\ 0 & if\ M_y > A_{new} \end{cases} \tag{5}$$

The percentage of new air conditioners which are VFD driven for a given 69kV bus, $\rho_{VFD,i}$, can be calculated as

$$\rho_{VFD,i} = \alpha_{VFD}\rho_i \tag{6}$$

The chosen penetration of VFD driven air conditioners among new air conditioners, α_{VFD}, is system-wide, not bus specific. The range of α_{VFD} was determined based on information from the utility's air conditioner rebate program data and consultation with local air conditioner installers. In the absence of residence sizes, houses are assumed to have the same air conditioner load on average. In reality, larger houses are more likely to have VFD driven air conditioners installed compared to smaller ones; feeders with larger houses would have a higher penetration of VFD driven air conditioners.

The percentage of new air conditioners which are VFD driven is calculated for each load bus modeled with CMPLDW for which home age information was provided, n, a total of 254 buses. However, it is helpful to know the total penetration of single-phase motors in the power system which are VFD driven, ρ'_{VFD}, which is calculated as

$$\rho'_{VFD} := \frac{\sum_{i=1}^{n} \rho_{VFD,i} Fmd_i P_{load,i}}{\sum_{i=1}^{n} Fmd_i P_{load,i}} \tag{7}$$

A. USING LD1PAC

Because the behavior of single-phase VFD driven air conditioners differs considerably from the one- or two-speed single-phase motors which are modeled by Motor D in CMPLDW, a separate and distinct model was used to model the VFD driven air conditioners. Consequently, the protection parameters of the VFD driven air conditioners could be modeled exactly; the Motor D parameters would not be tuned to account for VFD driven air conditioners. For this purpose, the single-phase performance model LD1PAC is used to model the VFD driven air conditioners.

Each load is represented in the load table of the power flow data file. In the dynamic data, there is one CMPLDW model which corresponds to each load. The use of more than one load model per load is not allowed by PSLF. Therefore, for each of the 254 load buses considered in the case studies, a second load in the power flow is created representing only the VFD driven air conditioners. Then an LD1PAC model is created in the dynamic data file corresponding to the VFD load in the power flow.

The reallocation of load from one represented by the CMPLDW model to load represented by the LD1PAC model requires editing the fractional load parameters in the CMPLDW model, *Fma*, *Fmb*, *Fmc*, *Fmd*, and *Fel*. This ensures that the total load – in megawatts – modeled as each type of three-phase motor, power electronic load, or static load remains equal to the base case. At each 69kV load bus, with the bus index i omitted in (8)-(13), the load and CMPLDW parameter values for the VFD penetration sensitivity studies are calculated as

$$P_1 = P_{1_0} - \rho_{VFD} Fmd_0 P_{1_0} \tag{8}$$

$$P_2 = \rho_{VFD} Fmd_0 P_{1_0} \tag{9}$$

$$F_{md} = \frac{P_{1_0} Fmd_0 - P_2}{P_1} \tag{10}$$

$$F_{ma} = \frac{P_{1_0} Fma_0}{P_1} \tag{11}$$

$$F_{mb} = \frac{P_{1_0} Fmb_0}{P_1} \tag{12}$$

$$F_{mc} = \frac{P_{1_0} Fmc_0}{P_1} \tag{13}$$

$$F_{el} = \frac{P_{1_0} Fel_0}{P_1} \tag{14}$$

The load P_2 is modeled in the dynamic data as LD1PAC. The LD1PAC parameters Vc_{1off}, Vc_{2off}, Vc_{1on}, and Vc_{2on}, are set to represent all P_2 as single-phase VFD driven air conditioners as described by the findings in [7]. Table 1 presents the key parameters used in LD1PAC to ensure that P_2 acts as the VFD driven air conditioner described in [7].

TABLE 1. LD1PAC parameters to model VFD driven air conditioners.

Vc_{1off}	Vc_{2off}	Vc_{1on}	Vc_{2on}	V_{Stall}	T_{Stall}
0.75	0.70	2.0	2.0	0.0	9999

B. USING CMPLDW ONLY

Using the LD1PAC model to model VFD driven air conditioners is burdensome; it requires editing load in the power flow, creating a new load in the power flow, adding a model to the dynamic data, and editing many parameters in the existing models. It is preferable to use only the CMPLDW model which is already in use.

Several attempts are made to match the results of simulations using the LD1PAC model. The VFD driven air conditioners are modeled using the power electronic load by adjusting parameters *Fmd* and *Fel* at each load bus (with load bus index i omitted) as

$$Fmd = Fmd_0 - \rho_{VFD} Fmd_0 \tag{15}$$

$$Fel = Fel_0 + \rho_{VFD} Fel_0 \tag{16}$$

The simulations using the LD1PAC model assumes that 0% of the load disconnected due to low voltage reconnects when voltage recovers. With the CMPLDW parameters used by the studied utility, 100% of power electronic load disconnected by low voltage reconnects when voltage recovers. The fraction of power electronic load which can reconnect at each load bus (with load bus index i omitted), *Frcel*, is calculated as a function of VFD driven air conditioner load added to the power electronic load and is given as

$$Frcel = Frcel_0 - \frac{\rho_{VFD} Fmd_0}{Fel} \tag{17}$$

IV. CASE STUDIES

A three-phase fault is applied on a 230kV bus, Bus 100, and cleared after five cycles, 0.08s. The 69kV buses supplied by Bus 100 constitute Zone 100. The bus voltages in Zone 100 are monitored, and the 12.47kV load bus with the lowest post-fault voltage is selected for further examination. The bus identified as having the lowest post-fault voltage is named as Bus 112L and corresponds to the 12.47kV substation low-side Bus 112, and Bus 169 at 69kV, on which the CMPLDW model is represented. Bus information is provided in Appendix A.

A. BASE CASE – 0% VFD AIR CONDITIONING

During the fault, voltage magnitudes on buses near the fault location are low, as expected. However, the bus voltages do not recover to their pre-fault values for several seconds until enough stalled single-phase motor load is shed. It takes 17.94s for the voltage magnitude at Bus 112L to recover to its pre-fault value. The fault causes undervoltage load shedding (UVLS) relays across fifty-one 69kV buses to operate, shedding a total of 126.86MW. The UVLS relay on Bus 169 operates at $t = 3.07$s. Thermal protection devices on single-phase motors at Bus 112L begin opening at $t = 8.05$s. Fig. 4 and Fig. 5 show the nearby bus voltages following the fault on Bus 100.

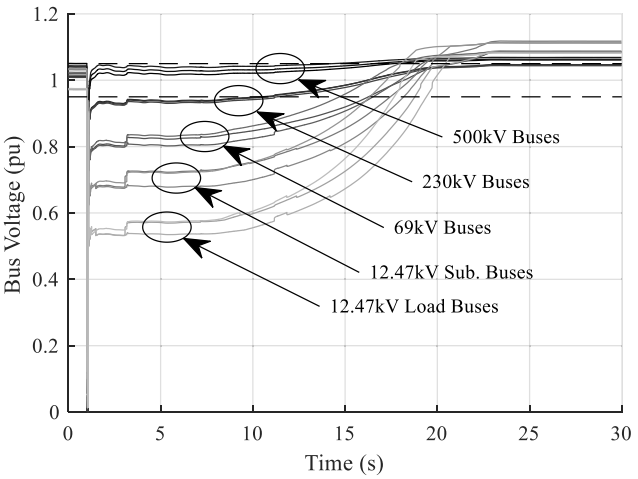

FIGURE 4. Nearby bus voltages following the fault on Bus 100.

Because motor speed is not calculated within the performance model, motor stalling is not an explicit output of the model. Therefore, a combination of Bus 169 active and

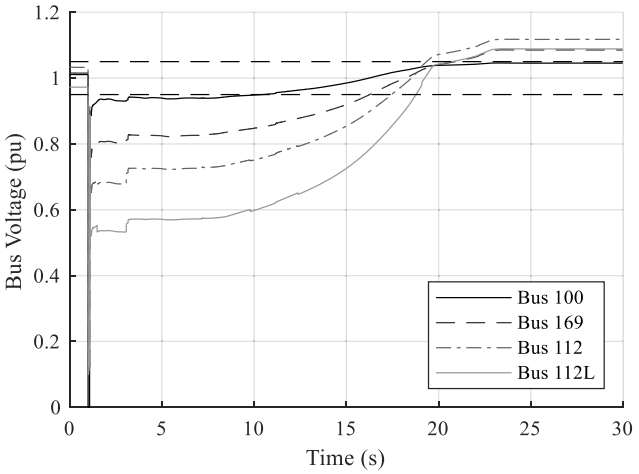

FIGURE 5. **Bus voltages following the fault on 230kV Bus 100.**

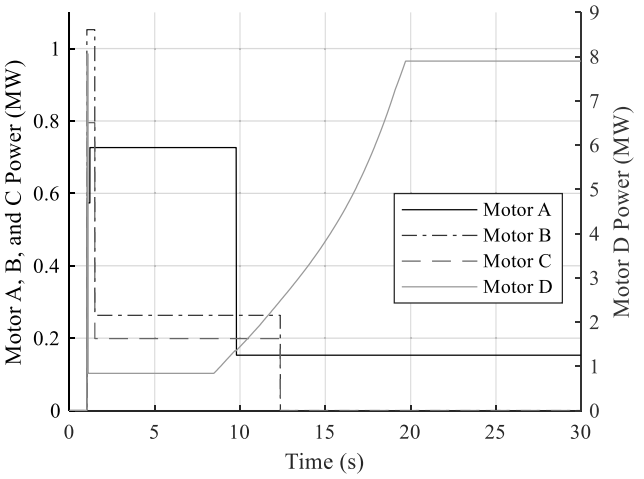

FIGURE 7. **Single- and three-phase motors tripped offline from Bus 112L, measured in MW.**

reactive power outputs and Motor D trip-status may be used to assess stalling.

Outputs from the CMPLDW model are fractional values representing the fraction of Motor D motors tripped by the four available tripping mechanisms: undervoltage relay operation, contactor dropout, load shedding, and thermal protection operation. The output of fractional values is not a perfect representation of the model dynamics, as at any given time the total fraction of motors tripped can exceed one, indicating that more than 100% of motors have tripped, an impossibility. The best conclusion drawn from the tripping of thermal protective devices is that all Motor D motors at Bus 112L stalled and eventually tripped.

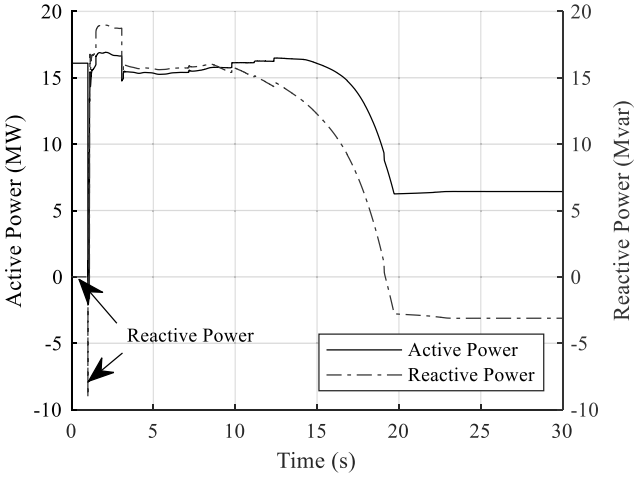

FIGURE 6. **Bus 169 active and reactive power following the fault on Bus 100.**

Bus 169 is operated at unity power factor. Therefore, before the fault, the reactive power is 0 Mvar. After the fault is cleared, the reactive power on the Bus 169 can be seen in Fig. 6 to increase significantly and exceed the active power on the bus. This indicates stalled motors connected to the bus drawing high reactive currents.

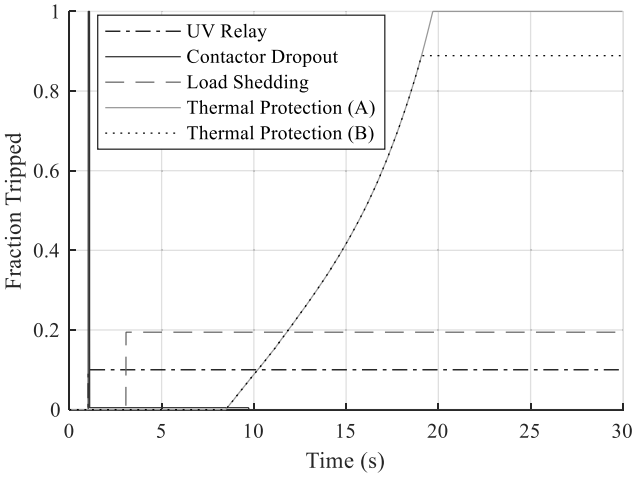

FIGURE 8. **Fraction of Motor D tripped.**

As stalled single-phase motors are disconnected from Bus 112L by thermal protection operation, as shown in Fig. 7 and Fig. 8, the reactive power on Bus 169 decreased below its pre-fault value, and bus voltage increased beyond its pre-fault value. The voltage of Bus 169 reached steady state when all the stalled single-phase motors were tripped.

Two additional case studies were performed by applying two different three-phase faults on 230kV buses in two additional zones with different load compositions and Motor D penetration levels. The results of the two additional case studies reinforce the findings for the fault applied at Bus 100. Information pertaining to the two additional case studies are found in Appendix A. The bus naming convention follows that of the case study presented.

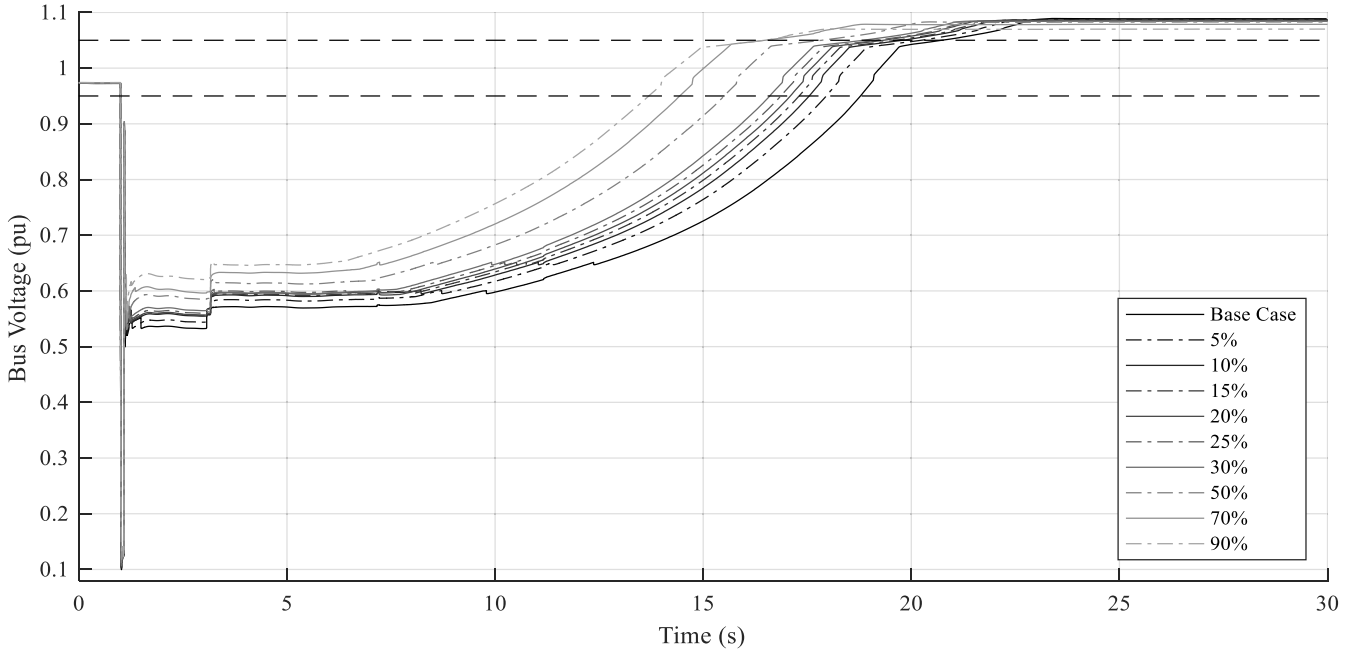

FIGURE 9. **Bus 112L voltages under varying penetration of VFD driven air conditioners modeled with LD1PAC.**

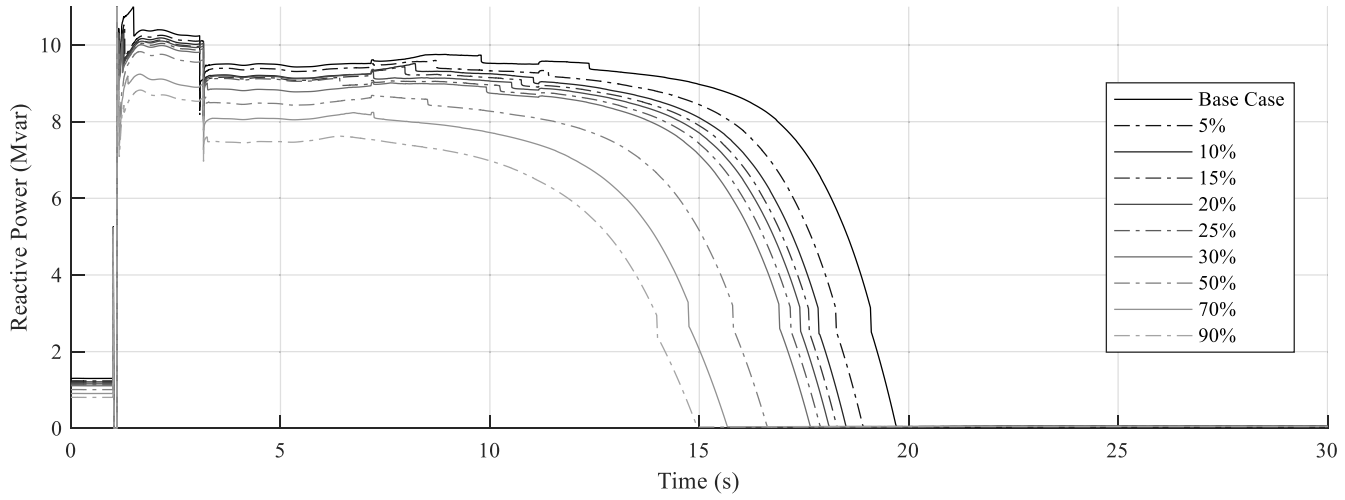

FIGURE 10. **Bus 112L Motor D reactive power under varying penetration of VFD driven air conditioners modeled with LD1PAC.**

B. VFD AIR CONDITIONER MODELING WITH LD1PAC

Following (1) – (14), various percentages – 5, 10, 15, 20, 25, 30, 50, 70, and 90% - of new air conditioner loads in the power system were modeled as VFD driven air conditioners using LD1PAC. The same three-phase fault was applied on Bus 100 and cleared after 5 cycles.

Fig. 9 shows that as VFD driven air conditioner penetration is increased, both the magnitude of the post-fault voltage drops, and the bus voltage recovery time is reduced. Because the post-fault voltage recovers sooner, there are fewer UVLS relay operations.

VFD air conditioners trip at much higher voltages due to VFD controller protection settings. The VFD air conditioners will not reconnect for several minutes while the VFD controller restarts. Shedding this load during and immediately after the fault results in post-fault bus voltage magnitudes being higher.

However, the one- and two-speed single-phase air conditioners, represented by Motor D in CMPLDW, still stall post-fault, and keep the post-fault bus voltage suppressed by drawing high reactive current. In the cases studied, all stalled Motor D motors tripped post-fault, as shown in Fig. 10.

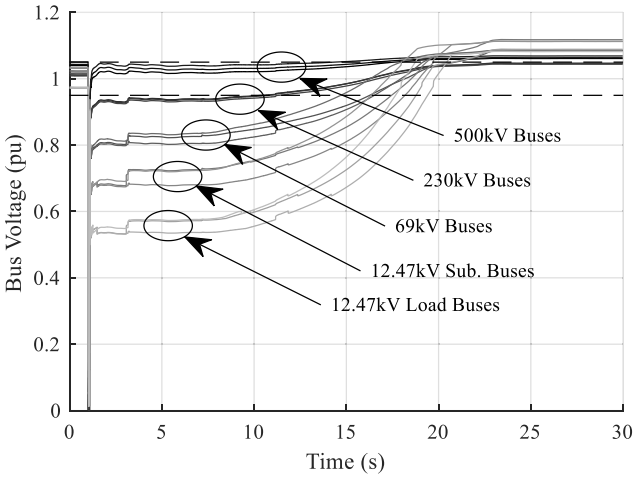

FIGURE 11. **VFD penetration at 15%: Bus voltages following the fault on Bus 100.**

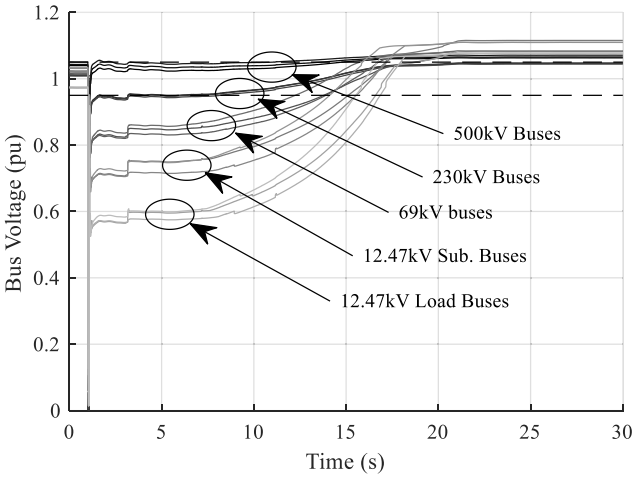

FIGURE 12. **VFD penetration at 30%: Bus voltages following the fault on Bus 100.**

Therefore, the severity of the FIDVR event was reduced, but not eliminated. Table 2 presents the bus voltage recovery time of the buses with the lowest post-fault voltages, and total load shed for the three faults studied as VFD air conditioner penetration is increased in the three different zones.

TABLE 2. **Post-fault voltage recovery time and total load shed.**

VFD Penetration of New ACs (%)	Voltage Recovery Time (s)			Total Load Shed (MW)		
	112L	212L	312L	112L	212L	312L
0	17.94	20.36	19.53	126.86	183.32	27.37
5	17.13	19.86	19.21	126.86	183.32	35.51
10	16.74	19.53	19.01	126.86	183.32	34.15
15	16.49	19.17	18.17	125.85	183.32	16.52
20	16.28	18.80	18.30	125.85	183.32	14.00
25	16.10	18.40	18.03	123.30	183.32	14.00
30	15.80	18.01	17.67	120.89	183.32	4.84
50	14.72	16.76	16.86	102.40	176.09	0
70	13.65	15.51	15.53	76.99	170.60	0
90	12.92	13.90	15.01	50.08	154.08	0

The improvement in post-fault bus voltage magnitude and recovery time is observed across bus voltages in the area surrounding the fault, as depicted in Fig. 11, 12, and 13..

C. VFD MODELING WITH CMPLDW ONLY

As described above, it is preferable to use only the CMPLDW model to decrease the data preparations and modeling effort required for representing VFD driven air conditioners. The 30% penetration of VFD driven air conditioners among new air conditioners case was chosen to use only CMPLDW to model VFD driven air conditioners.

The steps described by (1) – (8) and (15) – (17) were used to migrate a portion of single-phase motor loads representing VFD driven air conditioners from Motor D to the power electronic load. First, only the *Fel* power electronic load parameter was changed, using (14) and (15). Results are shown in Fig. 14. Then the *Frcel* parameter was changed to be a function of VFD driven air conditioner load added to the power electronic portion of CMPLDW, using (16). Results of this effort are depicted in Fig. 15.

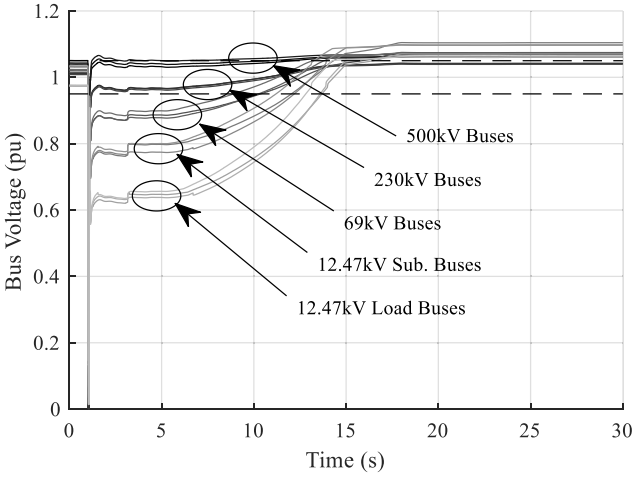

FIGURE 13. **VFD penetration at 90%: Bus voltages following the fault on Bus 100.**

It is apparent that editing the *Frcel* parameter to be a function of VFD driven air conditioner load added to the power electronic load does not yield more desirable results but increases modeling burden for the power system planner. It is shown in Fig. 16 that even when tested on the simulations with 90% VFD driven air conditioner penetration among new air conditioners, changing only the *Fel* parameter results in satisfactory results; the general shape of the voltage recovery curve is preserved, as is the voltage recovery time. This cannot be said for the simulations where *Frcel* is changed per (16). Fig. 17 shows a far more optimistic voltage recovery time.

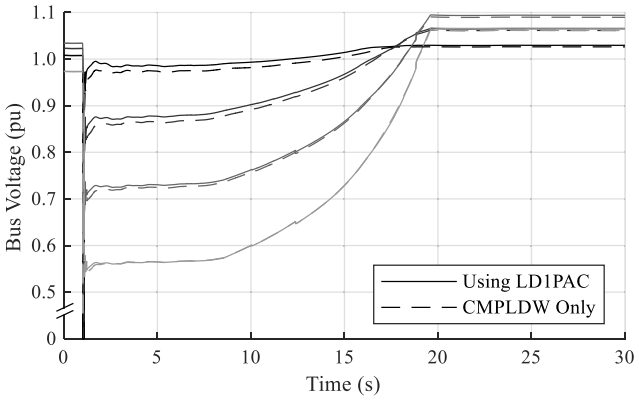

FIGURE 14. VFD penetration at 30%: Bus voltages following the fault on Bus 100 modeled with LD1PAC and CMPLDW only changing the *Fel* parameter.

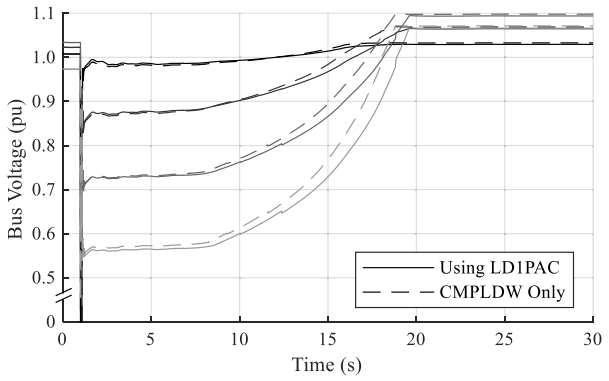

FIGURE 15. VFD penetration at 30%: Bus voltages following the fault on Bus 100 modeled with LD1PAC and CMPLDW changing the *Fel* and *Frcel* parameters.

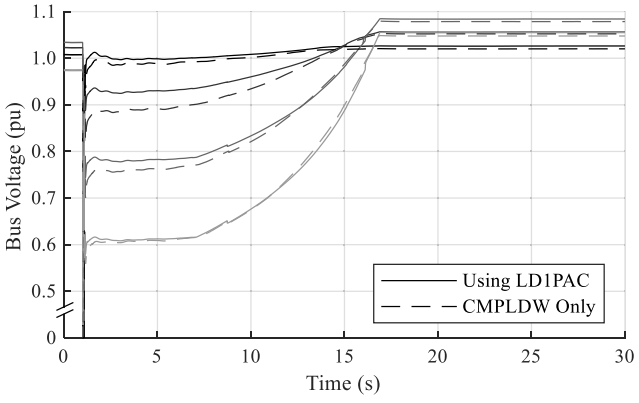

FIGURE 16. VFD penetration at 90%: Bus voltages following the fault on Bus 100 modeled with LD1PAC and CMPLDW only changing the *Fel* parameter.

Therefore, only changing the *Fel* and *Fmd* parameters within CMPLDW is necessary for capturing the effect of modeling a portion of single-phase air conditioners as VFD driven for planning studies.

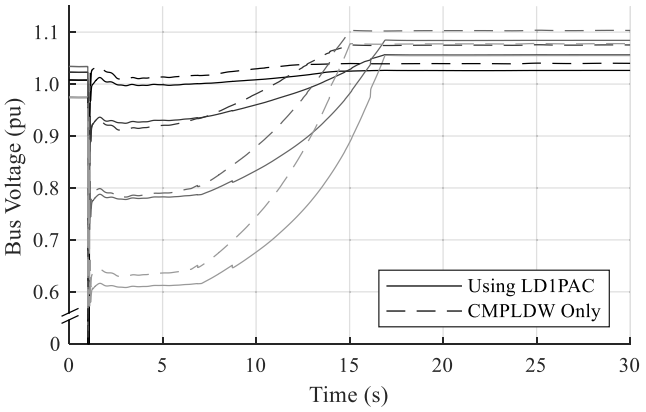

FIGURE 17. VFD penetration at 90%: Bus voltages following the fault on Bus 100 modeled with LD1PAC and CMPLDW changing the *Fel* and *Frcel* parameters.

V. CONCLUSION

This paper presents a simple method for modeling VFD driven air conditioners as the power electronic load within the CMPLDW model and shows that increasing the penetration of VFD driven air conditioner load leads to reduced severity of FIDVR events. The simulations of three case studies showed that as the percentage of new air conditioners which are VFD driven increases, the voltage sag following the fault is less severe, and the time for the voltage to recover to the pre-fault value is shortened. There are also fewer operations of UVLS relays as the penetration of VFD driven air conditioners increases, resulting in fewer customers being adversely impacted by the fault. The increase in VFD driven air conditioners improves post-fault conditions but does not eliminate the FIDVR events from occurring.

The utility whose system was studied in this paper had available information on the age of the homes on their 69kV sub-transmission feeders, and air conditioning rebate information. However, VFD driven air conditioner penetration sensitivity studies can be performed using other information which is available to the utility to establish ρ_{VFD} or ρ'_{VFD}.

Information about FIDVR events when VFD air conditioners are modeled can enhance power system planning and facilitate the design of corrective actions for FIDVR events or provide insight to customer programs for offering rebates to customers installing VFD driven air conditioners.

APPENDIX A

See Tables 3 and 4.

TABLE 3. Monitored zones.

Zone	Number of Load Buses	Active Load (MW)	Reactive Load (Mvar)	Motor D Load (MW)
100	15	207.1	7.99	47.25
200	19	207	7.69	217.93
300	12	272.6	0	119.53

APPENDIX B

Sample code used for both the CMPLDW and LD1PAC models used is provided below. Only the parameters listed

TABLE 4. 69kV buses with lowest post-fault voltage.

Bus	Residential Load Composition (%)	*Fmd*	Active Load (MW)	Motor D Load (MW)
169	81.3	0.4567	16.10	7.35
269	82.9	0.5470	20.29	11.10
369	82.7	0.6080	33.2	20.19

in the Nomenclature were changed during studies, otherwise the parameters used in the sample code remained unchanged.

```
cmpldw 11111 "BUSNAME" 69.00 "1 ": #9 mva=-1.25 "bss"
0.0 "rfdr" 0.04 "xfdr" 0.0 "fb" 0.75/
"xxf" 0.08 "tfixhs" 1.0 "tfixls" 1.0 "ltc" 0.0 "tmin"
0.9 "tmax" 1.1 "step" 0.00625 "vmin" 1.025 "vmax" 1.04
"tdel" 30.0 "ttap" 5.0 "rcmp" 0.0 "xcmp" 0.0/
"fma" 0.05 "fmb" 0.086 "fmc" 0.065 "fmd" 0.4567 "fel"
0.081/
"pfel" 1.0 "vd1" 0.7 "vd2" 0.5 "frcel" 1.0 /
"pfs" -0.996 "p1e" 2.0 "p1c" 0.415 "p2e" 1.0 "p2c"
0.585 "pfrq" 0.0/
"q1e" 2.0 "q1c" -0.5 "q2e" 1.0 "q2c" 1.5 "qfrq" -1.0/
"mtypa" 3.0 "mtypb" 3.0 "mtypc" 3.0 "mtypd" 1.0/
"lfma" 0.75 "Rs" 0.04 "Ls" 1.8 "Lp" 0.12 "Lpp" 0.104/
"Tpo" 0.095 "Tppo" 0.0021 "H" 0.1 "etrq" 0.0/
"vtr1" 0.65 "ttr1" 0.1 "ftr1" 0.2 "vrc1" 1.0 "trc1"
99999.0 "vtr2" 0.5 "ttr2" 0.02 "ftr2" 0.75 "vrc2" 0.6
"trc2" 0.05/
"LFmb" 0.75 "Rs" 0.03 "Ls" 1.8 "Lp" 0.19 "Lpp" 0.14
"Tpo" 0.2 "Tppo" 0.0026 "H" 0.5 "etrq" 2.0 "vtr1" 0.55
"ttr1" 0.02 "ftr1" 0.2 "vrc1" 0.65 "trc1" 0.05 "vtr2"
0.45 "ttr2" 0.02 "ftr2" 0.6 "vrc2" 0.55 "trc2" 0.0500/
"LFmc" 0.75 "Rs" 0.03 "Ls" 1.8 "Lp" 0.19 "Lpp" 0.1400
"Tpo" 0.20 "Tppo" 0.0026 "H" 0.1 "etrq" 2.0 "vtr1"
0.55 "ttr1" 0.02 "ftr1" 0.2 "vrc1" 0.65 "trc1" 0.05
"vtr2" 0.45 "ttr2" 0.02 "ftr2" 0.6 "vrc2" 0.55 "trc2"
0.05/
"LFmd" 1.0 "CompPF" 0.98 "Vstall" 0.4 "Rstall" 0.1
"Xstall" 0.1 "Tstall" 0.032/
"Frst" 0.2 "Vrst" 0.95 "Trst" 0.3 /
"fuvr" 0.1 "vtr1" 0.6 "ttr1" 0.02 "vtr2" 1.0 "ttr2"
9999.0 "Vc1off" 0.5 "Vc2off" 0.4 "Vc1on" 0.6 "Vc2on"
0.5 "Tth" 15.0 "Th1t" 0.7 "Th2t" 1.9 "Tv" 0.025

ld1pac 11111 "BUSNAME" 69.00 "2 ": #9 mva=-1.25 "pul"
1.0 "tv" 0.02 "tf" 0.05 "CompPF" 0.98 "Vstall" 0.0
"Rstall" 0.1 "Xstall" 0.1 "Tstall" 9999.0 "LFadj" 0.0
"Kp1" 0.0 "Np1" 1.0 "Kq1" 6.0 "Nq1" 2.0 "Kp2" 12.0
"Np2" 3.2 "Kq2" 11.0 "Nq2" 2.50 "Vbrk" 0.0 "Frst" 0.2
"Vrst" 0.95 "Trst" 0.3 "CmpKpf" 1.0 "CmpKqf" -3.3
"Vc1off" 0.75 "Vc2off" 0.7 "Vc1on" 2.0 "Vc2on" 2.0
"Tth" 15.0 "Th1t" 0.7 "Th2t" 1.9 "fuvr" 0.025 "uvtr1"
0.1 "ttr1" 0.6 "uvtr2" 0.02 "ttr2" 1.0
```

REFERENCES

[1] North American Electric Reliability Corporation. (Feb. 2017). *Reliability Guideline Developing Load Model Composition Data*. [Online]. Available: http://www.nerc.com/pa/RAPA/rg/ReliabilityGuidelines/Reliability_Guideline_Load_Model_Composition_-_2017-02-20.pdf

[2] D. Kosterev *et al.*, "Load modeling in power system studies: WECC progress update," in *Proc. IEEE Power Energy Soc. Gen. Meeting, Convers. Del. Electr. Energy 21st Century*, Pittsburgh, PA, USA, Jul. 2008, pp. 1–8, doi: 10.1109/PES.2008.4596557.

[3] *PSLF User's Manual, V21.1_07*, Gen. Electr. Int., Schenectady, NY, USA, 2019.

[4] *Load Component Export Tool (LCET), V3.1 (3002015441)*, Electr. Power Res. Inst., Palo Alto, CA, USA, 2019.

[5] P. Entingov. (Sep. 2019). Load model data tool (LMDT). Pacific Northwest National Laboratory. [Online]. Available: https://svn.pnl.gov/LoadTool

[6] North American Electric Reliability Corporation. (Nov. 2016). *Technical Reference Document Dynamic Load Modeling*. [Online]. Available: https://www.nerc.com/comm/PC/LoadModelingTaskForceDL/Dynamic%20Load%20Modeling%20Tech%20Ref%202016-11-14%20-%20FINAL.PDF

[7] A. Gaikwad, "Technical update on load modeling (3002013562)," Electr. Power Res. Inst., Palo Alto, CA, USA, Tech. Rep. 3002013562, 2018.

[8] P. Mitra, D. Ramasubramanian, A. Gaikwad, and J. Johns, "Modeling the aggregated response of variable frequency drives (VFDs) for power system dynamic studies," *IEEE Trans. Power Syst.*, vol. 35, no. 4, pp. 2631–2641, Jul. 2020, doi: 10.1109/TPWRS.2020.2966820.

[9] P. Mitra, "Technical reference on the composite load model (3002019209)," Electr. Power Res. Inst., Palo Alto, CA, USA, Tech. Rep. 3002019209, 2020.

[10] Petro Home Services. *HVAC Packaged Unit vs. Split System: Differences, Benefits, & How to Choose*. Accessed: Apr. 22, 2020. [Online]. Available: https://www.petro.com/resource-center/hvac-packaged-unit-vs-split-system

[11] Comprehensive Energy Services. (Mar. 2016). *When to Retrofit RTUs With Variable Frequency Drives (VFD)*. [Online]. Available: https://www.cesmechanical.com/ces-hvac-blog-home/when-to-retrofit-a-rtu-with-a-variable-frequency-drive-vfd

[12] B. Telker. Should you be adding a VFD on every packaged rooftoop unit? CFM Distributors. [Online]. Available: https://rc.cfmdistributors.com/helpful-tips/adding-vfd-every-packaged-rooftop-unit/

[13] Western Electricity Coordinating Council. (Jan. 2015). *WECC Composite Load Model Specifications*. [Online]. Available: https://www.wecc.biz/_layouts/15/WopiFrame.aspx?sourcedoc=/Reliability/WECC%20

[14] US Department of Energy. *Central Air Conditioning*. Accessed: Apr. 7, 2020. [Online]. Available: https://www.energy.gov/energysaver/central-air-conditioning